Flexural Behavior of Reinforced Concrete Beams layers with Silica Fume and Steel Fiber

Manal kademAbdullah
University of Thi-Qar
Iraq – Thi-Qar
Manalkadhum36@utq.edu.iq

Dr. Ali k. Al-Asadi
University of Thi-Qar
Iraq – Thi-Qar
alazharco.2005@utq.edu.iq

ABSTRACT

In this paper study, Nine beam samples with measurements of 1150 x 200 x 120 mm were prepared to examine the bending behavior of reinforced concrete (SRC,SRFC and SFRCH) beams exposed to flexural .All tested beams have the same rectangular section (W x H) of 1150 x 200mm. The span of the beams is 1000mm . Two Ø10 mm longitudinal reinforced have been provided at top and bottom. In addition, stirrups reinforcement of Ø10@50mm have been added to assure a pure flexural failure. Steel reinforcement has been designed and provided to allow the beams to fail under reinforcement failure scenario.. Letters S , F, SP "N.C," "SRC,SFRC and SFRCH refer to the silica fume ,steel fiber, Superplaciticizer ,normal control, beams with silica fume ,steel fiber and beam with layers respectively. silica and steel fiber were added to form S8F1 beam as a layers with thickness (H) corresponding to 1.5cm ,3cm, 6cm, 9cm, 12cm and 20cm. Figure 4-1 shown the beam specimens used as layers .Table 3 shows the proportion of concrete mix of the current study. For the lowest layer of C35 grade concrete in this investigation, we utilized concrete mixtures with 8% silica fume and 1% steel fiber, and for the upper layer, we used concrete mixtures with 8% silica fume and 0% steel fiber. The ideal thickness of the beam layers was S8F0H12, which improved the outcomes of the ultimate state as the thickness of the SFRCH layer increased. Given that S8F0H6 is greater than S8F1, we must utilize a beam whose thickness is 6 cm higher than S8F1 in order to be more cost-effective. Table 4 shown the beam specimens used as layers with Reference beam N.C, S8F0 and S8F1

Keywords: Silica Fume, steel fiber Compressive Strength, Split strength stress strain in compression ,ductility ,stiffnes, flexural behavior and Slump

I.Introdation

For many infrastructure constructions, concrete is a typical building material. On sometimes, concrete technology makes rapid advancements. Due to the extensive use of concrete materials in building, engineers and scientists are driven to keep coming up with new, high-quality products that are strong and long-lasting. [1] Concrete that is strong and durable enough will save maintenance expenses and hence satisfy economic material standards. A creative choice is to combine several components with various physical and chemical qualities to create a high-quality

building material like concrete. Concrete reinforced with steel fibers and filled with silica fume is the substance produced in this investigation. In order to form concrete, these two ingredients will be combined [2]. Concrete has a lengthy history as one of the most widely used construction materials. Since its introduction in the mid-nineteenth century, reinforced concrete (RC) has introduced new, more cost-effective engineering structural styles to buildings, as well as new design and calculation theories and building procedures. It does, however, have certain intrinsic flaws,[3] such as limited tensile strength, ductility, and energy absorption. These disadvantages become more substantial as concrete strength increases. As a result, numerous specialists are working on strategies to improve tangible habits. Adding a tiny fraction (0.5 percent -2 percent in volume in most circumstances) Adding steel fiber to regular concrete when mixing with cement and aggregates is an effective way to boost its performance. In the 1960s, research on steel fiber reinforced concrete first started. [4] Following years of research, it is commonly believed that this type of concrete may greatly enhance several concrete characteristics. The function of fibers in fiber reinforced concrete is to prevent fractures from forming. Aggregates and fibers both carry the weight in the early phases of loading, with aggregates serving as the main carriers. The principal carriers after breaking are the fibers that are closest to the cracks. The fiber reinforced concrete can bear more weight and distortion until a particular volume percentage has been reached until the fibers are ripped or pulled out. Because of this, fiber reinforced concrete is more ductile and has more compressive and tensile strength than conventional plain reinforced concrete. [5] One of the most used indirect methods is the Force Activity Index (SAI). In this procedure, suspected pozzolan is substituted for a standard amount of Portland cement, and the strength development is compared to that of a mix made entirely of Portland cement. The SAI is then determined by dividing the strength of the cement mixture by the strength of the pozzolanic mixture. Since both tests combine suspected pozzolan with Portland cement, it is not unexpected that the Frattini test (R2 = 0.86) and the indirect SAI test (R2 = 0.86) correspond well. [6]

II.Steel Fibers

strengthened mostly with prestressed strands. SFs that fall under the category of high-volume parts (more than 2% of the volume of concrete) have exceptional mechanical Characteristics and can be used without other constant reinforcement, but because of processing and cost limitations, these composite materials are frequently only appropriate for extremely specialized applications. Fig.1shows Hook end Steel Fibers.

Fig1.: Hook end Steel Fibers

III.Steel fiber benefits

Numerous variables, containing type, form, length, cross section, strength, fiber content, matrix strength, mix design, and concrete mixing, affect the good effects of SFs in concrete. Fig.2 illustrates typical load-curves of deflection for FRC and normal concrete. The following are some benefits of including SFs in traditional reinforced concrete (RC) members: [7]

1- By increasing the tensile strength of the matrix, SFs increase the flexural strength of the concrete.

2- The post-cracking strength and restraint of the cracks in the concrete are due to the crack bridging mechanism of SFs and their capacity to transmit loads equally throughout the matrix.

3. Make the concrete more ductile. Chapter One of the general introduction 10.

4- Compared to traditional RC, SFRC is more serviceable and long-lasting. The sole drawback of SFRC is that it requires more vibration to make it workable, which reduces its workability and accelerates the stiffening of

fresh concrete caused by the addition of SFs. This problematic may be partially resolved by the use of lately advanced high range superplasticizers, which not only make SFRC easier to work with but also conserve the plasticity of the mixture for a longer period of time. [8]

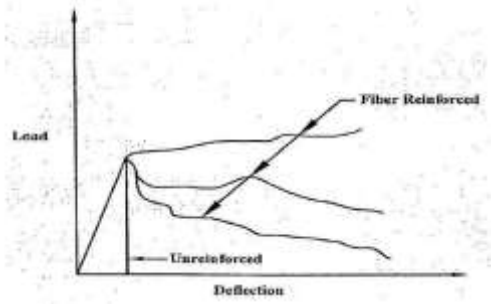

Fig 2: Curves of Load-Deflection for Normal and Fibrous Concrete. (ACI 544.IR, 1996)

IV. Silica Fume

Microsilica, sometimes referred to as silica fume, is an amorphous polymorph of silicon dioxide and silica (amorphous). It is an extremely fine by-product of the manufacture of silicon and ferrosilicon alloys, and each of its 150 nanometer-diameter spherical particles is a separate atom. The pozzolanic component in high-performance concrete is where it is most frequently used. It can occasionally be disordered with fumed silica. However, silica fumes and fumed glass are produced using separate processes, and silica fumes have different particle properties and application areas. [9] Silica fume (fine silica) has been known as a pozzolanic combination capable of increasing concrete's mechanical qualities as well as its chemical durability. Silica fume is increasingly being employed in the construction of high economic strength concrete and/or chemical resistant concrete in many regions of the world. Silica fume has been utilized as a cement replacement in ordinary strength concrete in Canada from its introduction to achieve a desired 28-day compressive strength. It is currently employed in the form of manufactured cement or mixed cement. A type 10SFsilica-fume mixed cement is now being marketed by Canada's two largest cement companies. Its dose is always less than 10% by weight of the cement, whether it is used in product form in the concrete factory or combined with Portland cement. In reality, Canadian Standard A23.6 allows for a maximum dosage of 10%. [10] Fig.3 explain shape of silica fume.

V. Properties & Advantages Silica Fume

The average diameter of the spherical particles in silica fume, which is an ultrafine material, is 0.15 m in diameter. In comparison to a conventional cement particle, it is approximately 100 times smaller. Depending on the level of densification in the silo, the bulk density of silica fume ranges from 130 kg/m3 (unidentified) to 600 kg/m3 (densified). Silica fume typically has a specific gravity of 2.2 to 2.3Both the BET method and the nitrogen adsorption method can be used to determine the specific surface area of silica fume. It typically ranges from 15,000 to 30,000 m2/kg. [11] Table 1 lists the physical and chemical properties of silica fume.

Fig.3 : shapes of Silica Fume

The advantages of Silica Fume can be summarized in the following points

1. The characteristics of fresh and hardened concrete are improved by silica fume.
2. Silica fume inhibits bleeding and segregation.
3. Long-term durability
4. Because of the reduced bleeding, the finishing procedure is efficient.
5. High compressive strength in the early stages.
6. High flexural strength and elasticity modulus
7. Excellent bonding strength.
8. It's good for bulk concreting since it reduces thermal cracking. [12]

Table 1: The Physical and Chemical characteristics of Silica fume

Properties	Silica Fume
Calcium oxide (CaO)	0.1
Specific gravity	2.2
Mean grain size (µm)	0.1
Specific area (cm2/gm)	200000
Colour	Light to Dark Grey
Silicon dioxide (SiO2)	96.0
Aluminium oxide (Al2O3)	0.1
Iron oxide (Fe2O3)	0.6
Magnesium oxide (MgO)	0.2
Sodium oxide (Na2O)	0.1
Potassium oxide (K2O)	0.4
Loss on ignition	1.7

VI. Material

All materials (Fine aggregate, Coarse aggregate, Cement, and Steel reinforcements) have consistent properties through the current study. The materials were tested at the Labs of College of Engineering - University of Thi-Qar. Hooked-end steel fiber as shown in Fig.4(b) has been used in this study. It has been added to the concrete mixtures at a volume fraction of one (Vf). Their characteristics are shown in Table 2, together with silica fume at 8% of the cement's weight. Almas bars with a diameter of 10 mm for longitudinal reinforcement and 10 mm for transverse reinforcement were used to strengthen all beams in accordance with BS 4449-2009. (stirrups). In this study, hooked-end fibers produced by SPI Muhendislik ve Dis Ticaret Ltd Sti were used. Steel's Table 2 Properties. In this procedure, type-II sulphate-resistant Portland cement was employed, along with ASTM C150. High-range water-reducing (HRWR) TYPE G, a high-performance superplasticizer that complies with ASTM C494 standards, was utilized to increase the workability. In this investigation, coarse aggregate that complied with ASTM C33 and Each particle of natural sand has a maximum size of 4.75 mm Cement is substituted in part with silica fume. Simply said, silica fume is a pozzolanic substance with high strength and low permeability. as shown in Fig.4(a) Additionally, Superplasticizers have high water reduction rates that produce high densities and are utilized to promote workability. as shown in Fig.4(c) Table 3 lists the mix proportions that were employed in this investigation. For around 10 minutes, all elements were combined in a concrete mixer. A steel reinforcing bar was then placed horizontally within the wooden molds before the concrete mixture was poured into them. Steel reinforcement is employed, as seen in Fig. 5.

(a)silica fume (b) steel fiber

(c) Superplasticizer

Fig.4: Hooked-end fiber , silica fume and Superplasticizer used (a) and (b)

Fig 5: The steel bar has been tested and used

1 Experimental program and Preparation of test specimens :

1.1 Mix Design

For all beam samples, a 35 MPa compression strength had been specified for the concrete mixture. To determine the design strength, numerous trial combinations were tested experimentally. Weight was used to determine all materials. The specified concrete mix (400 kg/m3 of cement, 1150 kg/m3 of gravel, 700 kg/m3 of sand, and 0.425 of w/c ratio) was used to pour three concrete cubes. The percentage of the present study's concrete mix is shown in Table 3. For the purpose of evaluating the compressive strength, split tensile strength, and flexural behavior of R and C, respectively, IS standard 150mm Cubes, 150mm X 300mm cylinder, and 120mm X

200mm X 1150mm were cast from each combination. Then, these cubes were evaluated after 28 days, with each test being repeated in triplicate. Table 4 shows Details and description of the beam specimens. Fig.6 beam specimens used as layers

Table 2: shows properties of steel fiber

Details	Diameter (mm)	Length(mm)	Aspect Ratio	Tensile Strength Mpa
Hooked-Ends Fiber	0.5mm	30mm	60	≥2800

Table 3: the proportion of concrete mix of the current study

Cement (Kg/m3) C	Coarse aggregate (Kg/m3)	Fine aggregate (Kg/m3)	Water (Kg/m3)
400	1150	700	168

Table 4: Details and description of the beam specimen layers:

NO.	Name of beams	Thickness of lower layer cm	Thickness of upper layer cm	Lower layer	Upper layer	w/c	Sp%
1	S0F0N.C	-----	-----	-----	-----	0.425	0.4
2	S8F0	-----	-----	-----	-----	0.425	0.4
3	S8F1	-----	-----	-----	-----	0.425	0.4
4	S8F0h1.5	1.5	18.5	S8F1	S8F0	0.425	0.4
5	S0F0h3N.C	3	17	S8F1	N.C	0.425	0.4
6	S8F0h3	3	17	S8F1	S8F0	0.425	0.4
7	S8F0h6	6	14	S8F1	S8F0	0.425	0.4
8	S8F0h9	9	11	S8F1	S8F0	0.425	0.4
9	S8F0h12	12	8	S8F1	S8F0	0.425	0.4

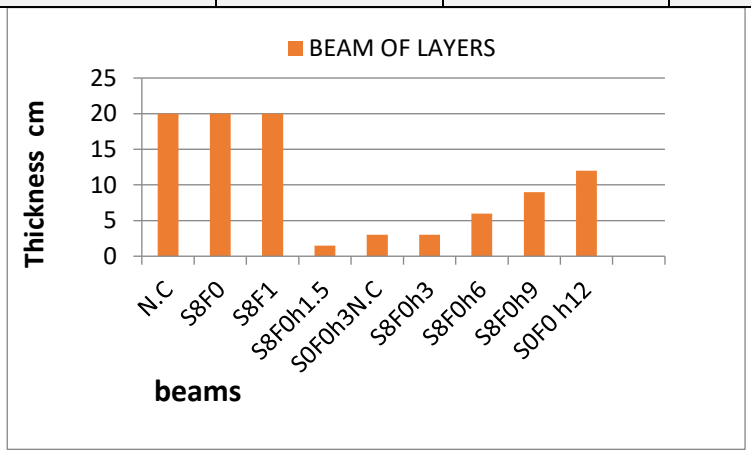

Fig.6: beam specimens used as layers

1.2 Workability

The slump test has been carried out experimentally to get the workability of fresh concrete e according to specifications of ACI 211.1-91(Reapproved 2009) [13]. The consistency of the mixtures was evaluated by a slump test. the results are shown in Table 5.As shown ,the slump values of mix of concrete S0F0N.C,S8F0 and S8F1. The most concrete mix expected to reduce workability due to adding fibers which is the mix with high dosage of hooked ends steel fibers of 1% by volume. The addition of silica fumes a partial for cement into the specimens with steel fiber decreased the Workability. With the addition of steel fiber and silica fume to the mix, the slump was reduced. Additionally, the drop of the concrete decreased. Due to silica fume's high water absorption level, which drastically reduces the workability of concrete, even adding a lot of superplasticizer to high-strength concrete doesn't always result in the desired workability. Superplasticizer has therefore been utilized to obtain satisfactory workability outcomes. The slump test is depicted in Fig 7.

Table 5 shows slump of N.C,S8F0an S8F1

No.	Specimen	Slump test mm
1	BMS0F0N.C	110
2	BMS8F0	90
3	BMS8F1	40

(a) (b) (c)

Fig.7 slump test; (a) slump for N.C, (b) slump for S8F0and (c) slump for S8F1

1.3Mechanical properties

1.3.1Compressive strength

To determine the compressive strength of the concrete, three cube specimens (150 mm) were cast for each mix and tested in accordance with BS 1881-116 [14]. As seen in Fig.8), tests were conducted utilizing a digital compression machine with a (3000 KN) capacity. After casting and water curing for 28 days, the tests were carried out.

Fig.8: Digital compression machine used

1.3.2 Compression Stress-Strain Test

The cylinders of (150x300) mm were used to evaluate the stress-strain relations. Before testing, a digital dial gage attached to metal rings which were mounted 120 mm from the top and the bottom of the specimen used to measure the displacement on the cylindrical. The metal rings were fixed in a way that preserves the measuring device and allows for lateral deformations that occur to the cylinder during the test process. Strain calculations were found by dividing the change of length registered in the digital dial gage on the original length for the specimen. A metal cup was used at the top and bottom end of the cylinder to ensure uniform load distribution. The test was carried out in accord with ASTM C 39/C39M [14], as shown in Fig.9.

Fig.9: Compression stress-strain test

1.3.3 Splitting tensile test

The test was carried out on ten cylinder specimens (S0F0, S8F0and S8F1) in diameter of (150 mm) and 300mm length were cast for ten mix and tested according to BS 1881-116 [14] to obtain the tensile strength of the concrete. Tests were carried out using a digital compression machine of (3000 KN) capacity as shown in Fig.10. After casting and water curing for 28 days, the tests were carried out. The cylinder is positioned horizontally between the compression testing machine's loading surfaces, and the load is applied until the cylinder fails. Plywood is utilized as packing material to prevent any unexpected loads. The testing apparatus's platens shouldn't be permitted to spin during the test in a direction perpendicular to the cylinder's axis. The following equation is used to compute the split tensile strength:

$$\boldsymbol{fct = 2P / (\pi LD)} \qquad \textbf{-------- Eq. (3.1)}$$

Where:

fct: Splitting tensile strength, MPa.

P: Ultimate Applied load, N.

D: Diameter of the cylinder, mm

L: Length of the cylinder, mm

Fig,10: Digital The split tensile strength machine used

1.4 Flexural Testing Machine, Matest

All specimens are tested in a universal testing machine as shown in Fig.11 (a) with a capacity of 150 kN at the structure's laboratory in the building of Engineering college at University of Thi-Qar. As illustrated in Fig. 11 the test beams are simply supported throughout a span of 1000 mm while resting on a rigid steel frame that is loaded with four-point stresses (b).The load is applied vertically and monotonically increasing. Readings of the applied load and central deflection are recorded at regular intervals during the tests. As indicated in Fig.11(c), an unique holder placed a digital dial gauge at the midpoint of the tested beams to measure Deflection. Table 6 lists the dial gauge's properties as stated by the manufacturer.

Table 6: Properties of Dial Gage Used

Properties Value	Properties Value
Maximum Capacity (mm)	50
Accuracy 0.01	0.01
Type	Digital

(a) (b) (c)

Fig.11 (a) Flexural testing machine , (b) test of beam and (c) The digital dial gauge used

2 .Experimental results and discussion

2.1 Mechanical properties:

2.1.1 Compressive strength and Split Tensile of Concrete

Table 7 displays the results of the compression strength (fcu) and split tensile (fct) tests conducted on cubic and cylinder specimens of N.C., S8F0, and S8F1. For cubes, the sample weight was recorded prior to the test. Figure 12 compares the compressive strength and split tensile strength of N.C., S8F0, and S8F1 after 28 days of curing. It is clear that these properties improved for S8F0 and S8F1 in contrast to N.C .This result is directly related to silica fume's filling activity, which increases the cement paste-aggregate interface's binding strength .The concrete's splitting tensile strength (fct) and compressive strength (fcu) both improved by (11 and 48 and 9 and 51.1) percent, respectively. These findings imply that the adding of steel fiber and silica fume to concrete significantly growths the concrete's capacity to withstand compression stress. This may be clarified by the fact that steel fibers serve as crack arrestors while silica fume improves the compressive strength of the transition zone in concrete. In order to reduce segregation, bleeding, and improve flowability, these materials are crucial. Besides that, the simultaneous addition of steel fiber and silica fume to the aggregate-paste bond has been shown to increase the splitting tensile strength. The tensile strengths are markedly improved when the vacancies are first filled with silica fume, but the gains diminish at increasing levels. The fracture patterns of cubics

(compressive strength) and cylinders (split tensile strength) of N.C., S8F0, and S8F1 are depicted in Figures 13 and 14, respectively.

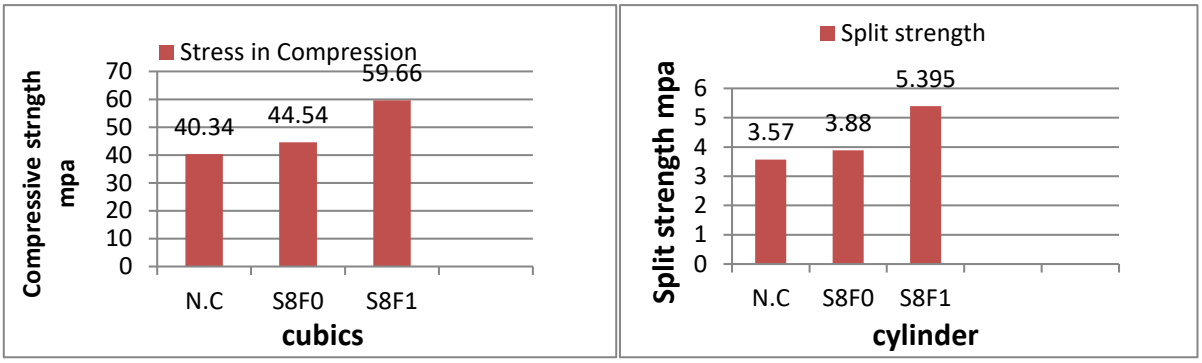

(a) Compressive for N.C,S8F0 and S8F1 **(b) Split strength for N.C,S8F0 and S8F1**

Figure 12: Comparison of compressive and split strength between the N.C, S8F0 and S8F1 used.(a)and(b)

(a)N.C **(b) S8F0** **(c)S8F1**

Figure (13): (a),(b) and (c) , crack pattern of cubics (compressive strength) of N.C, S8F0 and S8F1

(a) N.C **(b) S8F0** **(c)S8F1**

Figure (14): (a),(b) and (c) , crack pattern of cylinder (split tensile strength) of N.C, S8F0 and S8F1

NO.	Name of beams	Silica fume%	Steel fiber%	Weight of Cubic (g)	Averages of Cubic Compressive Strength at 28 days (MPa) (fcu)	Split tensile mpa (fct)
1	S0F0N.C	0	0	8241	40.34	3.57
2	S8F0	8	0	8164	44.54	3.88

6	S8F1	8	1	8290	59.66	5.395

Table 7 Test results of mechanical properties of N.C,S8F0 and S8F1

2.1.2 Stress-Strain relation under compression of N.C, S8F0 and S8F1

Fig.16 shows the experimental stress-strain curves of the tested normal concrete (N.C) , S8F0 and S8F1 cylindrical specimens. The shape of the ascending part of the stress-strain curve for steel fiber reinforced concrete shows more linear and steeper behavior compared to normal concrete. Steel fibers reduce cracks growth in concrete under loading and consequently increases load resistance and decreases deformation demonstrate that adding silica fume to concrete that has steel fiber reinforcement improves the elastic modulus, with the increase being greater for steel fibers. The results obtained for stress- strain compression test given in Table`8, It can be noted the improvement in stress-strain behavior due to using silica fume with addition steel fibers .Table 8 shows stress compression of Concrete (S8F0 andS8F1) increased by (15% and 41 %), respectively compared with normal concrete N.C. Employing silica The link between the cement paste and aggregates becomes more solid as a result of fume, increasing the stiffness of the concrete. As a result, the presence of fine pozzolan particles raises the concrete's stiffness, improving elastic modulus. The graphic shows that while all specimens typically behave the same during the first step (linear stage), they behave differently at the final stage. Tables document the increases in compressive strength (8). Normal concrete cylinders collapsed in a brittle way after achieving their maximum strength, and the post-peak softening branch of their stress-strain curves could not be seen. However, the inclusion of the steel fibers reduced the elastic modulus of the concretes made only of silica fume. However, depending on the concrete's ductility, the addition of steel fibers tends to lower the material's elastic modulus. Fig.15 compares the fracture patterns of cylinders N.C, S8F0, and S8F1.

Table 8 Test results of Stress-strain of N.C, S8F0 and S8F1

NO.	Name of beams	Stress mpa
1	S0F0(N.C)	27
2	S8F0	31
3	S8F1	38.01

Fig.15: Comparison of the crack pattern N.C , S8F0 and S8F1 of cylinders

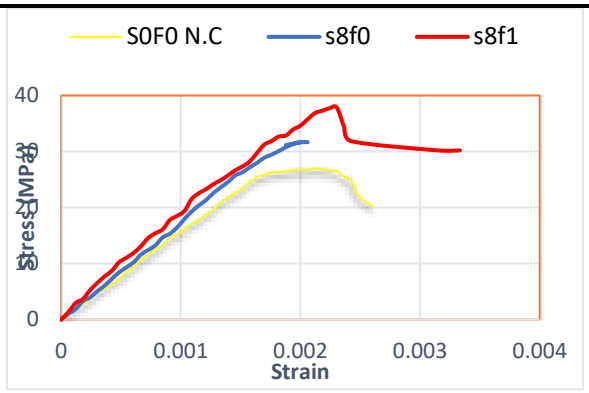

Fig.16 stress –strain curves for N.C,S8F0and S8F1

2.1.3Reference Flexural Results- Normal Control beam(N.C).

The curve resulting from the flexural test of the normal control beam (N.C) is drawn in Fig.18. The figure shows that the first crack was at the load of 20 and the corresponding deflection is 1.37mm as stated earlier in Table 9. The ultimate load and deflection, on the other hand, are 99.1kN and 9.77mm, respectively. As can be depicted from the figure, the yielding load and deflection cannot be determined directly from the figure, and therefore, yielding load and deflection have been determined to be 90kN and 6.42 mm using the method proposed by Park [15]and Pam et al. [16] discussed earlier. The deformation of the N.C continued until the maximum deflection of 12.47 mm. Deflection of the tested beams was monitored by using a digital dial gauge located at mid span of the tested beams by a special holder.

The deflection is measured at the midpoint of the tension surface of the tested beams (at the mid-span) by dial gauges . For each load increment, the readings are recorded from this gauge. In general, when the load increases, the deflection increases linearly in an elastic stage. The deflection increases with a higher rate after the cracks start appearing. The experimental values of the loads and corresponding deflection for the first crack ultimate and yield loading stages are shown in Table (9). After cracks have advanced in the beam, the curve of load-deflection is approximately linear up to the yielding of flexural reinforcement. Figure 17 and figure 18 shown cracks pattern and deflection curve of normal control beam. Respectively. , the specimens under bending generally were considered to experience three stages until failure: loading stage, cracking stage, and yield stage of steel bars.

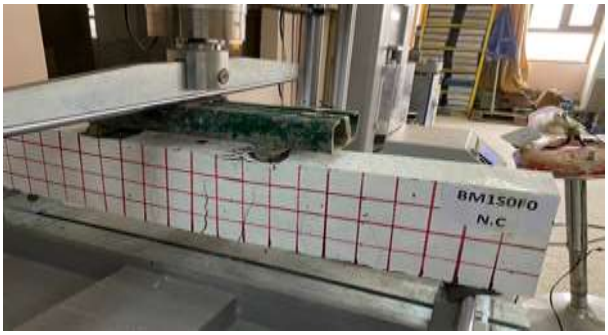

Fig17 : Cracks Pattern of N.C

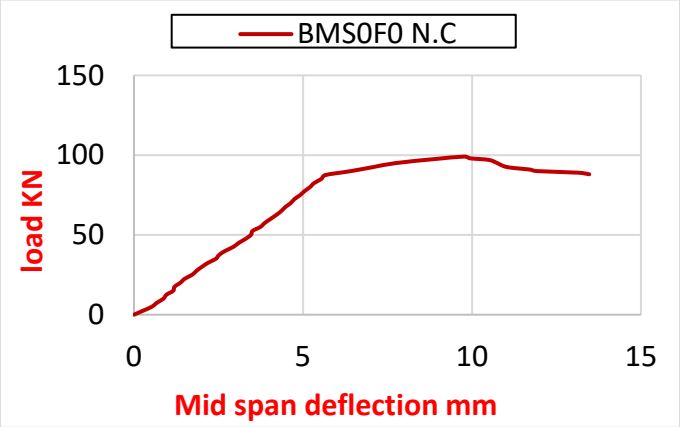

Fig.18: Load-deflection curve of normal control (N.C)

2.1.4 Crack patterns and mode of failure for N.C, S8F0 and S8F1.

When the tensile stresses in the concrete's extreme tension fiber surpass the rupture modulus, a crack forms in flexural members. In the middle part of the beam, the first noticeable crack was formed in the maximum bending moment region. In the beam normal control (N.C) that consists of ordinary concrete, it is noticed that the crack failure is in a straight line at the middle of the specimen, and the number of cracks was few, compared to beams that contain silica fume and steel fiber. The control beam failed by cracking and crushing of the concrete on the top surface. This type of failure referred to as flexural tension failure and this happens when the beam is under-reinforced. Concrete at the compression side of the beam is crushed by yielding steel reinforcement, which causes flexural stress failure. The initial fracture load of S8F0 and S8F1 significantly increased as compared to a normal control beam, as illustrated in fig. 20.

Furthermore, the adding of steel fiber led to a more diffused cracking pattern. In addition, there are many secondary cracks that are growing and developing out of the primary cracks. According to the observation of the crack pattern, the presence steel fiber showed improved performance in cracking control. An increase of steel fiber in the mix provided a very good ductility for this system with more hairline cracks in the bending zone appeared. This showed that the beams were able to resist a larger load by combining fibers with different properties and lowering the opening of cracks with the ultimate load. All reinforced concrete beams were failed in flexural. Modes of failure and the crack patterns of the tested beams as shows in Fig.19.

Fig.20 : Cracks Pattern of S8F0 and S8F1

Table 9: Flexural Tests Results of Beam Layers of SFRCH, N.C,S8F0 and S8F1

NO.	Name of beams	Cracking State pcr %pcr (KN) (KN)	Δcr (mm)	Yielding State Py %Py (kN) (KN)	Δy (mm)	Ultimate State Pu %Pu (kN) (KN)	Δu (mm)
1	S0F0N.C	20 0	1.37	90 0	6.42	99.1 0	9.77
2	S8F0	25 25	1.55	92 2.25	6.31	101.54 3	9.65
3	S8F1	33 65	2.05	101 12.2	6.73	110.15 11.2	10.67
4	S8F0h1.5	28 40	1.46	92.5 3	6.3	104.07 45	9.58
5	S0F0h3N.C	30 50	1.68	97 8	6.28	106.58 68	9.87
6	S8F0h3	32 60	1.84	99.5 11	6.36	108.92 89	10
7	S8F0h6	33 65	2.1	102 14	6.68	110.8 106	10.21
8	S8F0h9	35 75	2.35	104.89 17	6.94	113.7 132	10.82
9	S8F0h12	36 80	2.46	110.9 23.2	7.28	116.82 160	11.1

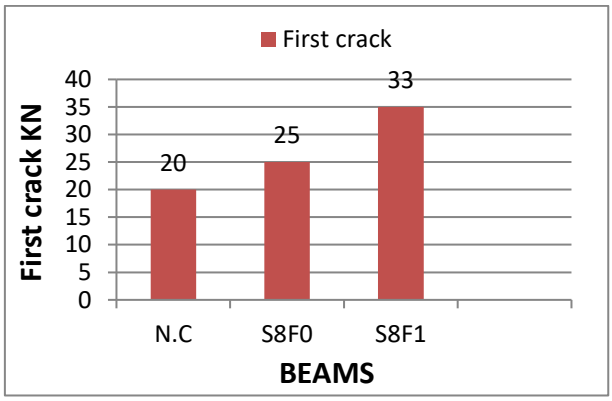

Fig.20: The first crack load of beams (a)N.C ,S8F0 and (b) S8F1

2.1.5 Flexural Results of SFRCH

The main variables investigated in this study of beam layers and the subsequent groups are the thickness of the SFRCH layer, which is located in the lower part of the beam's cross-section of S8F0h1.5, S0F0h3N.C, S8F0h3, S8F0h6, S8F0h9 and S8F0h12 the fiber volume fractions ,Fig.22 shows the load-deflection curves for SFRCH layer and compred it with N.C and S8F1 as documented from the investigational testing data. In general, the second portion indicates the yielding of the tensile reinforcing steel, and the third part depicts the linear behavior under a low applied load until the first crack load (Pcr). which, upon cracking of the tension zone of the beam, exhibits a continuous increase in both concrete compression and tensile stresses of the reinforcing bars;and the third part represents the yielding of the tensile steel, the extension and growth of the cracks until

failure of the beams. As compared to the flexural behavior of N.C, and S8F1 although all curves share approximately the same linearity from the initial loading stage up to the yielding stage, the superiority of this beams group have been revealed by improving both the ultimate load and mid-span deflection as shown by the quick visual reviewing of Fig.22. Such that improvement ascribes to the addition of 1.0% steel fiber at different thickness of HSFRC layer. Regarding the difficulty identified of the cracking state visually as stated earlier, the cracking loads of this beams layers have been determined experimentally to be 28kN, 30kN, 32kN, 33, 35 ,36 and 33 kN which recorded for each height for specimens (i.e., S8F0h1.5, SF0h3N.C, S8F0h6, S8F0h9, S8F0h12and S8F1 respectively). Also, crack deflections of this beam layers have been determined experimentally to be 0.1.46 mm, 1.68mm, 1.84mm, , 2.1,2.35 and 2.46 mm respectively which recorded for each layers , as well. As compared with N.C, It can be noted that cracking loads of beam layers increased for (S8F0h1.5, SF0h3N.C, S8F0h6, S8F0h9, S8F0h12and S8F1) increased by(40%,50%,60%,65%,75%,85%, and 65% respectively) compared with N.C. observed noticeable results in the First crack as the thickness of the SFRCH layer was increased.. Because both beams have provided for nearly results of cracking .Fig.21 explains first crack of SFRCH.

in Table 9 explains results of deflection of SFRCH. It can be noted that effect of thickness of beam on behavior of reinforced concrete To study the influence of thickness of beam on load-deflection relationship accurately, all other parameters must be kept constant and only the (thickness of beam) can be varied (1.5, 3N.C, 3S8F0, 6 , 9 ,12 and 20cm), it can be noticed that increasing the thickness of beams leads to increase in the deflection compared with normal control, This means that the deflection increases due to the increased thickness of beam. The completely SFRCH load deflection curves have an approximate slope that increases linearly with the initial crack load. The impairment of SFRCH compared to N.C. causes the curve to follow a divergent route after the initial crack load..Figure 22 shows load deflection curves relationship of SFRCH beams enhanced significantly with the increase thickness of beams. The deflection increased with increase in loads. These effected were more pronounced for SFRCH beams and larger deflections occur after yield stage and before failure , Finally, at the failure stage, all of the tested beams in this group exhibited the flexural-shear failure mechanismThe load against mid-span deflection curves are initially linear in form and slope. After cracks begin to form, the load-deflection response adopts a nonlinear shape with a changing slope, with the deflection increasing as the applied force increased..This significant improvement in cracking load and deflection may be explained by more steel fibers spanning the tested members' fractures, which would boost the fibers' bridging effect. Given that these cracks typically start at the tested beam's bottom fiber, where bending stresses are present, the thickness of the HSFRC layer also has no bearing in this situation. Figure 23 shows Cracks Pattern of SFRCH (beam layers)

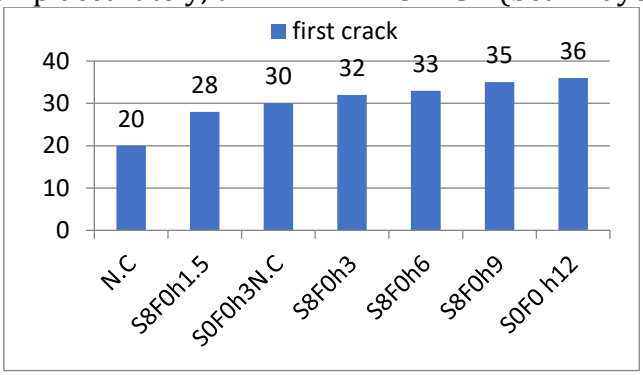

Fig.21: The first crack load of beams layers SFRCH

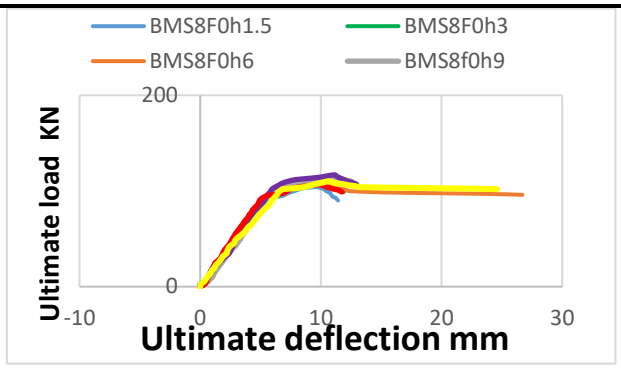

Fig.22: Ultimate Load vs. Ultimate deflection curve of layers beam

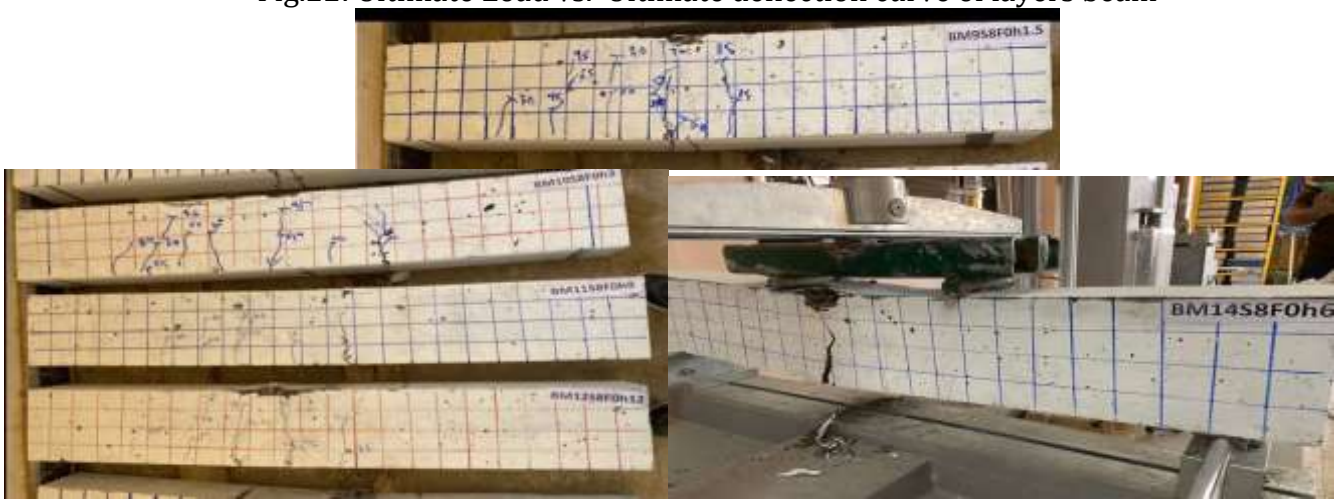

Figure (23) : Cracks Pattern of SFRCH (beam layers

2.1.6 Ultimate load of SFRCH, N.C,S8F0 and S8F1

As evidenced by the findings in Fig. 24, and Table 10 show the ultimate load for N.C,S8F0,S8F1and SFRCH and ultimate load of S8F0 and S8F1 higher than N.C due presence of silica fume and steel fiber. The beams layers recorded gradually enhancing results of ultimate state with uses of silica with fibers . according for beam layers .It can be noted that the improving in the ultimate load capacity for (S8F0h1.5, S0F0h3N.C, S8F0h3, S8F0h6,S8F0h9 and S8F0h12) increased by about (45% ,68%,89%,106%,132% and 160%) respectively, comparing to the N.C , Also, deflection ultimate of this beam layers have been determined experimentally to be 9.58mm, 9.87, 10mm, 10.21, 10.7 and 11.1mm respectively, which recorded for each beam layers , as well. As compared with N.C , This beams layers also recorded noticeable results of ultimate state with increasing thickness of SFRCH layer. The maximum value of the ultimate load is 116.82 KN for S8F0h12.Thus, the flexural performance of all specimens was found to be higher than that of the control specimen , also to discuss the results, a S8F0H6 higher than S8F1 beam and almost the same behavior , this means that the use of a layer thickness of 6 cm reduces the cost and is more economical . Concrete pumping is more effective when S and F are used, which lowers labor costs and improves safety. Ultimate load increases With the increase thickness of beam.. Finally, uses of steel fiber increases the ductility of beams as compared to those without steel fibers, increasing the number of cracks while reducing crack width. els was continuously monitored during the testing. The percentage of increase for ultimate load is calculated using the proposed Eq. 4-1 below:

$$\%Pu\ increase = Pu\ \%h - PuN.C\ Pu\ /100\%h - PuN.C \quad \text{Eq. 4-1}$$

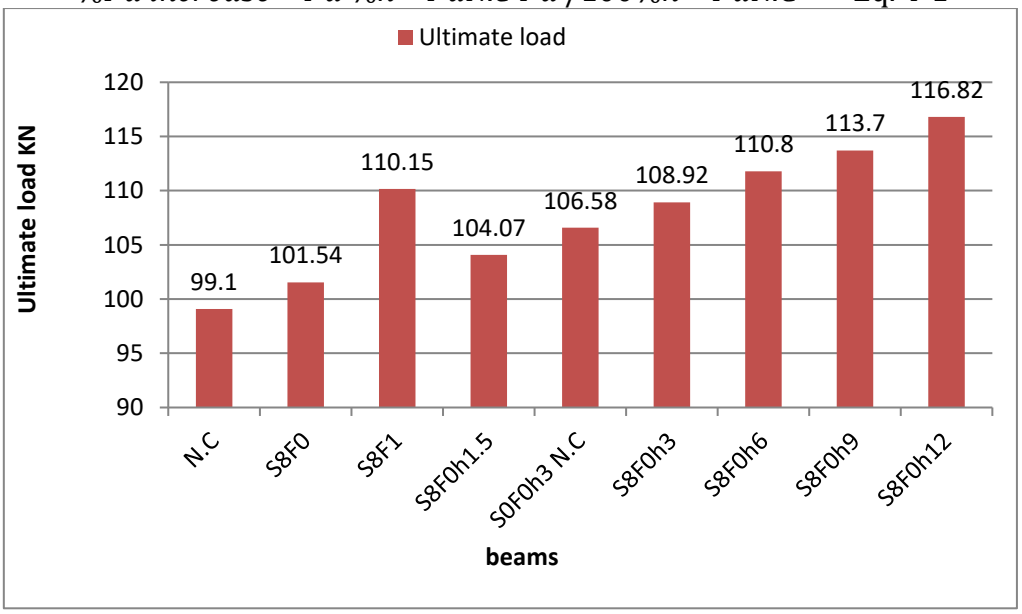

Fig.24: Ultimate load of specimens N.C,S8F0,S8F1 and SFRCH

Table 10: Result Ultimate load of N.C,S8F0,S8F1and `SRFCH

NO.	Name of beams	Ultimate load KN	The Increase in Ultimate load (%)
1	S0F(N.C	99.1	0
2	S8F0	101.54	3
3	S8F1	110.15	11.2
4	S8F0h1.5	104.07	45
5	S0F0h3N.C	106.58	68
6	S8F0h3	108.92	89
7	S8F0h6	110.8	106
8	S8F0h9	113.7	132
9	S8F0h12	116.82	160

2.1.6 Ductility of SFRCH, N.C,S8F0 and S8F1

The ductility (μ) of the beam layers with N.C ,S8F0 and S8F1 has also been calculated and recorded in Table 11 to find the influence thickness of beam on their behavior. The ductility index had been calculated using Eq. 4-2. Concrete pumping efficiency is increased by using S and F, which lowers labor costs and improves safety.

$$\mu = \delta u / \delta y \quad \text{Eq. 4-2}$$

Table11: Ductility of N.C,S8F0,S8F1and SRFCH

NO.	Name of beams	Deflection at midspan mm	Deflection at yield mm	Ductility
1	S0F0(N.C)	9.77	6.42	1.522
2	S8F0	9.65	5.95	1.62
3	S8F1	10.67	6.73	1.6
4	S8F0h1.5	9.58	6.13	1.56
5	S0F0h3N.C	9.87	6.28	1.57
6	S8F0h3	10	6.36	1.57
7	S8F0h6	10.21	6.61	1.54
8	S8F0h9	10.82	6.94	1.56
9	S8F0h12	11.1	7.28	1.524

2.1.7 Post-Cracking Stiffness and Cracks Patterns of SFRH

Post-cracking stiffness (Kcr) of the tested specimens have been calculated and recorded in Table 12 to find the influence thickness of beam layers on their behavior. And It has been calculated by using Eq. 4-3 as suggested in the literature [17].

$Kcr = Py - Pcr\ /\delta y - \delta cr$ Eq. 4-3

Where

Kcr is the crack stiffness.

Py is the yield load.

Pcr is the cracking load.

δy is the defection corresponding to the yield load.

δcr is the defection corresponding to the cracking load.

It can be seen from Table 12 the cracking stiffness index generally increased with increased thickness of beam compared normal control. The cracks pattern and intensity have a limited change, where the divisions of cracks have mainly concentrated in the SFRCH zone as shown in Fig.24

Table 12: Post-cracking stiffness of N.C,S8F0,S8F1and HFRCH,

NO.	Name of beams	Py	Pcr	Δy.	Δcr	Post-cracking stiffness Kc (kN.mm)	The increase in stiffness (%
1	S0F0(N.C)	90	20	6.42	1.37	13.86	0
2	S8F0	92	25	5.95	1.55	15.23	10
3	S8F1	101	33	6.73	2.05	14.53	2.5
4	S8F0h1.5	93	28	6.1	1.46	14	0.01
5	S0F0h3N.C	96	30	6.28	1.68	14.35	3.5
6	S8F0h3	99.5	32	6.36	1.84	14.93	7.7
7	S8F0h6	102	34	6.61	2.1	15.1	9
8	S8F0h9	104.89	35	6.94	2.35	15.23	10
9	S8F0h12	110.1	36	7.28	2.46	15.40	11.11

VIII Conclusion

1 The goal of this study is to investigate the flexural behavior and crack distribution of RC beams. There were a total of nine different types of beam that were cast, and each specimen had a different thickness of beam with a constant percentage of steel fiber at 1% and silica fume at 8%. the flexural performance of S8F0 and S8F1 was found to be higher than that of the normal control .

2 the mixing of concrete with steel fiber and silica fume was improved the Resistance and mechanical characteristics of the concrete by increasing the resistance of members deflection against loads, ductility and flexural resistance

3-While the increasing in Silica Fume ratio has an important influence on the compressive strength as well as the bonding between the steel fibers and concrete.

4-The ultimate mid-span deflection was increased with increased thickness of beam layers because of the increasing in steel fiber ratio will make the SSRC more ductility and can resist more deflections before arriving to the ultimate load (increasing the beam resistance). These features will develop the structural members and allow to concrete to give sign warn before failure instead of sudden collapse. The deflection ductility is compared to N.C andS8F1 beams and SRCFH beams show the enhanced properties.

5- It was noticed that the failure of beams was not sudden, which means the mode of failure of beam was flexural mode. There was a decrease in workability (slump) as the replacement level increase. Increasing steel fiber dosage resulted in the decrease of workability of SRCFH.

6-. The adding of silica fume is improving the bond strength of concrete and decreasing the permeability of concrete

7- By adding silica fume to concrete in order to achieve greater strengths, concrete becomes more brittle; nevertheless, the inclusion of steel fibers in concrete creates a ductile concrete structure, increasing the concrete's ability to absorb energy.

8- With an increase in steel fiber content, concrete gains weight density. In comparison to regular concrete, the addition of silica fume greatly boosts compressive strength. 28 days later, the compressive strength had increased to its maximum.

9- With the addition of steel fiber, the compressive strength increases for the 28-day period with the highest silica fume content.

10- In all specimens for beam layers , It was shown that raising the SFRCH beam's layer thickness resulted in a higher ultimate load.

References

1. Shannag, M. J. (2000). High strength concrete containing natural pozzolan and silica fume. Cement and Concrete Composites, 22(6), 399–406.
2. Almusallam AA et al, (2004). Effect of silica fume on the mechanical properties of lowquality coarse aggregate concrete. Cement & Concrete Composites 26(7):891–900.
3. C.X. Qian and P. Stroeven, Development of hybrid polypropylene–steel fibre reinforced concrete. J Cem Concr Res, vol. 30, pp. 63– 69, 2000.
4. S.J. Pantazopoulou and M. Zanganeh, Triaxial tests of fibre-reinforced concrete. J Mater Civ Eng, vol. 13, pp. 340–348, 2001.
5. Mehta, P.K. (1987). "Natural pozzolans: Supplementary cementing materials in concrete". CANMET Special Publication. 86: 1–33.
6. Snellings, R.; Mertens G.; Elsen J. (2012). "Supplementary cementitious materials". Reviews in Mineralogy and Geochemistry. 74: 211–278.
7. Chen, Y.Y. and Hwang, C.L. (2001). Study on Electrical Resistivity and Chloride Ion Penetrability Behavior of Concrete Material. Journal of the Chinese Civil and Hydraulic Engineering.13(2), p. 293
8. Grzybowski, M. & Shah, S. P. 1990. Shrinkage cracking of fiber reinforced concrete. ACI Materials Journal, 87
9. Amitava Roy, Nicholas Moelders, Paul J. Schilling, and Roger K. Seals (2006).

—Role of an Amorphous Silica in Portland Cement Concrete. ASCE Mat. J (18) 747-753.

10. [10] David B. McDonald, A. S. AI-Gahtani, Rasheeduzzafar, A. A. AI-Mussallam, Yacoub M. Najjar, and Imad A. Basbeer (1996). —Discussion of Resistance of Silica-Fume Concrete to Corrosion-Related Damages. ASCE Mat. J(8) 177-178.
11. [11] Detwiler, R.J. and Mehta, P.K., "Chemical and Physical Effects of Silica Fume on the Mechanical Behavior of Concrete" ACI Materials Journal, Vol. 86, No. 6, NovemberDecember, 1989, pp. 609-614..
12. [12] Bayasi, Z., and Zhou, J., "Properties of Silica Fume Concrete and Mortar" ACI, Material Journal, V.90, No.4, Jul-Aug, 1993, p. 349.
13. [13] S. J. M.-b. ASTM, "Standard specification for deformed and plain carbonsteel bars for concrete reinforcement," 2009.
14. [14] BS 1881:Part 116:1983-Testing concrete. Br Stand Concr. 1983;BSI BS*LBB.
15. [15Test Method for Compressive Strength of Cylindrical Concrete Specimens; C39/C39M-20; ASTM International: West.
16. [15] Park, "Ductility Evaluation From Laboratory and Analytical Testing," Bibliography R-9 Proceedings of Ninth World Conference on Earthquake Engineering, vol. VIII, no. Tokyo-Kyoto,JAPAN, 1988,
17. [16] H. J. Pam, A. K. H. Kwan, and J. C. M. Ho, "Flexural strength and ductility of reinforced concrete beams," Proceedings of the Institution of Civil Engineers: Structures and Buildings, vol. 152, no. 4, pp. 361–369,
18. [17] I. H. Yang, C. Joh, and K. C. Kim, "A Comparative Experimental Study on the Flexural Behavior of High-Strength Fiber-Reinforced Concrete and High-Strength Concrete Beams," Advances in Materials Science and Engineering, vol. 2018, 2018.